Evaluation of Waste-Derived Materials for CO_2 Capture to Enhance H_2 Yield from the Gasification of Urban Wastes

Despina Vamvuka*, Konstantinos Kyriakidis, Spyridon Karvounis, and Antonios Stratakis

School of Mineral Resources Engineering, Technical University of Crete, Chania, Greece
Email: dvamvouka@tuc.gr (D.V.); kkyriakidis@tuc.gr (K.K.); skarvounis@tuc.gr (S.K.); astratakis@tuc.gr (A.S.)
*Corresponding author

Manuscript received October 24, 2025; revised December 10, 2025; accepted January 9, 2026; published May 25, 2026

***Abstract*—This study focuses on the production of syngas rich in hydrogen from the gasification of municipal solid wastes, using widely available waste materials to capture CO_2 emissions. The experimental set-up involved a fixed-bed reactor combined with a thermal analysis-mass spectrometry system, allowing for comprehensive evaluation of the process. Building waste materials, coal fly ashes and agricultural wastes were investigated as CO_2 sorbents. Key outcomes, studied under varying operating conditions, included characterization of the feedstocks, fuel conversion, composition and energy content of product gas, yields of syngas and hydrogen and energy recovery. The results showed that without the addition of sorbents the concentration of hydrogen in the product gas was 39 mol%, while that of CO_2 was 35 mol% at 750 °C. When building wastes were used as a CO_2 sorbent, the hydrogen content in the resulting gas mixture peaked at 80.8 mol% and 91.1 mol% of CO_2 was captured. The poorest performance was obtained in the case of olive kernel ash as a sorbent. The use of all waste materials analyzed could provide a sustainable waste management option, with both environmental and economic benefits.**

***Keywords*—waste materials, carbon dioxide capture, steam gasification, municipal solid wastes**

I. Introduction

The growing global generation of Municipal Solid Waste (MSW), primarily driven by rising population numbers, increasing urban development, and shifts in consumption habits, has become a critical environmental issue. The accumulation of about 24 billion tons of MSW each year around the world [1], with an estimated annual rate of about 3.4 billion tons [2], poses serious threats to ecosystems and human health, highlighting the urgent need for efficient and sustainable waste management solutions. While many countries have implemented recycling systems, primarily targeting plastics and metals [3, 4], the recovery of energy from MSW, particularly due to its substantial organic content, offers a highly appealing approach amidst global energy challenges and growing support for circular economy initiatives.

Of the various waste-to-energy technologies, gasification is considered a more eco-friendly option compared to incineration, offering higher energy efficiency and greater flexibility in both input materials and the range of useful outputs [5–8]. Steam gasification, in particular, produces a hydrogen-rich syngas that can be used for heat and power generation (in engines, turbines, boilers, fuel cells), as well as for the production of fuels and chemicals [8–11]. Still, this method faces several technical hurdles, including the need for high operating temperatures, the formation of tar that contaminates the gas, and the release of CO_2, a major greenhouse gas. To combat tar production, strategies such as catalytic reforming and the use of 2-stage pyrolysis-gasification systems have demonstrated their effectiveness [12–14], while calcium-based sorbents are often used to capture CO_2 emissions, but also to boost hydrogen output [15, 16]. Producing low-carbon hydrogen from MSW through gasification appears to be a promising and scalable industrial solution [17, 18].

Despite the potential advantages of MSW gasification, research in this area remains underdeveloped. The majority of past work has focused on air gasification, which often results in lower energy efficiency and reduced calorific value of the produced gas [19–22]. For the air gasification of MSW in a fixed bed downdraft gasifier, at an equivalence ratio of 0.32, the lower heating value of the gas was 4.42 MJ/m^3 and H_2/CO = 0.72 [23], whereas at an equivalence ratio of 0.45 these values were 4.6 MJ/m^3 and 1.09 respectively [24]. When using a fixed bed updraft gasifier at an equivalence ratio of 0.3, the concentration of H_2 in the product gas was 6.65 mol%, the lower heating value of the gas was 2.58 MJ/m^3 and the H_2/CO = 0.66 [8]. Steam gasification of MSW remains relatively unexplored. To assess the thermal decomposition of common MSW components, thermogravimetric analysis coupled with mass spectrometry and kinetic modeling was performed [25]. The average composition of the resulting gas from high temperature gasification (>1100 °C) of MSW has been reported to be 37–39 vol% H_2, 40–41 vol% CO, 10–12 vol% CO_2, 4 vol% H_2O and 4–5 vol% Ar [26]. The steam gasification of refused-derived fuel at 900 °C and a steam/refused-derived fuel mass ratio of 1, in a fixed bed reactor, generated approximately 36 mol% H_2, 32 mol% CO, 8 mol% CH_4, 22 mol% CO_2 and 2 mol% CxHy [20]. Various catalysts have been used to reduce tar and obtain a cleaner syngas output containing more hydrogen. At about 900 °C, calcined olivine resulted in a H_2 content of 37.7 mol% in the syngas [27], however, Fe_2O_3/Al_2O_3 and zeolite catalysts produced syngas with a H_2 mole fraction of 83.7% [28]. The addition of calcium-based additives has been shown to decrease tar and CO_2 production in the syngas. With a Ni-CaO-TiO_2 catalyst at a catalyst/MSW = 0–1 and a temperature of 700–850 °C, the H_2 content of the gas, from the steam gasification of MSW in a fixed bed reactor, increased from 35 mol% to 57.7 mol% [29]. For a mixture of MSW and wood residue, at a ratio of 1:1.25 with the addition of CaO at 2:1 and 0.92:1, a thermodynamic simulation predicted 68.8 mol% H_2/kg feed and a CO_2 capture efficiency of 92% [22]. In some investigations, waste marble powder was utilized as a CO_2 sorbent at a molar ratio with MSW of 1 or 0.7, resulting in a product gas with 28 mol% or 49.4 mol% H_2 respectively, and around 30 mol% CO_2 at 750 °C [5, 30]. In another case

involving food waste, increasing the molar ratio of CaO to feedstock from 0.5 to 2, significantly raised hydrogen output, reaching a value of 70.5 kmol/h [15]. However, when gypsum was introduced at a 1:1 mass ratio, at 800 °C, syngas production dropped by 50% [16].

From the preceding discussion, the majority of previous investigations reported the air gasification of MSW in fluidized bed systems, or the catalytic reduction of tar. There are relatively limited studies on the steam gasification of MSW in fixed bed systems, integrated with CO_2 capture. Principally, sorbents in the form of lime have been used. Therefore, current research focuses on addressing the knowledge gap in the steam gasification of MSW, using novel sorbents for CO_2 capture to enhance hydrogen yield, offering a pathway to reduce landfill dependency and mitigate associated environmental impacts. The innovative aspects of this work are the use of unprocessed MSW, as well as the utilization of widely available waste materials, to capture CO_2 emissions during the thermochemical conversion process, such as urban construction wastes, fly ashes generated from coal power plants and agricultural wastes. These local materials have not been examined before as in situ CO_2 sorbents, and their use provides a sustainable waste management option with both environmental and economic benefits. The experimental set-up involved a fixed-bed reactor integrated with a thermal analysis–mass spectrometry system. MSW was firstly characterized by proximate and ultimate analyses, calorific value, pore volume, specific surface area and chemical functional groups. Sorbent materials were characterized by chemical and mineralogical analyses. The feedstock was then pyrolyzed in the reactor, the products were quantitatively analyzed and their energy content was determined. MSW char was gasified in the reactor up to 900 °C, either alone or mixed with each CO_2 sorbent. The results, including fuel conversion, composition and energy content of product gas, yields of syngas and hydrogen and energy recovery, were investigated under different reaction temperatures, steam-to-fuel ratios, as well as types and quantities of CO_2 sorbents.

II. Materials and Methods

A. Raw Materials

Municipal Solid Waste (MSW) used as the gasification feedstock was collected once per month over a one-year period from DEDISA, the municipal waste management facility serving Chania in Western Crete Prior to sampling, recyclable fractions such as plastics, metals and glass were removed by the facility, resulting in a mixture consisting roughly of 50% food residues, 30% paper-based materials, 12% lignocellulosic biomass, and 8% inert matter. The waste was air-dried, then size-reduced with a cutting mill and sieved to obtain particles smaller than 1 mm for the gasification tests and below 500 μm for fuel characterization.

4 materials rich in calcium were selected as CO_2 sorbents. Building demolition Waste (BW), largely derived from limestone bedrock and concrete plaster, was gathered from construction works at the Technical University of Crete. This material was pulverized using a planetary ball mill and sieved to sizes under 100 μm. Fly Ash (FA) originated from the Ag. Dimitrios lignite-fired power station in Western Macedonia and was supplied by the Public Power Corporation. Olive Kernel Ash (OKA) was produced in the laboratory from olive kernels obtained from an olive mill in Western Crete, and an MSW-derived Ash (MSWA) was also prepared. All sorbents underwent calcination at 950 °C for 2 h. Post-calcination, they were stored for approximately 10 days in a humidified quartz container to convert CaO to $Ca(OH)_2$—the active phase responsible for capturing CO_2 [31, 32].

Additional sorbent variants included a Silicon-Enriched Fly Ash (FASI) and a Potassium-Rich Olive Kernel Ash (OKAK). These were incorporated to evaluate how Si and K affect hydrogen production during steam gasification of the fuel.

B. Materials Characterization

Fuel characterization—proximate analysis, ultimate analysis and calorific value—was carried out in accordance with European Standard CEN/TC 335. A Quantachrome Autosorb 1Q-C-MP system was used to measure pore structure and specific surface area. Samples were degassed at 200 °C under vacuum for 1 h before analysis, and nitrogen adsorption isotherms were obtained between relative pressures of 0.015 and 0.32 using the Brunauer-Emmett-Teller (BET) method. The devolatilized MSW fuel was further examined with a Perkin Elmer Spectrum 100 Fourier Transform Infrared spectrometer (FTIR). Functional groups were identified across 400–4000 cm^{-1} with a spectral resolution of 4 cm^{-1}.

For the CO_2 sorbents, elemental composition was measured using a Bruker AXS S2 Ranger X-Ray Fluorescence (XRF) system, while crystalline phases were identified with a Bruker AXS D8 Advance X-Ray Diffractometer (XRD), supported by DIFFRAC Plus software and the Crystallography Open Database.

C. Experimental Equipment and Procedure

A schematic of the experimental system used for the gasification trials is presented in Fig. 1. Initially, raw MSW was subjected to pyrolysis in a fixed-bed reactor, under a nitrogen flow of 200 mL/min. The temperature was increased to 600 °C at 10 °C/min and held for 30 min. This pretreatment was used to enhance fuel reactivity and to improve syngas purity in the subsequent gasification step. During pyrolysis, condensable vapours were captured in ice-cooled traps, weighed, and centrifuged to isolate the bio-oil fraction.

Elemental analysis of the bio-oil was performed using a Thermo Fisher Flash 2000 CHNS analyzer, and its Higher Heating Value (HHV) (MJ/kg) was computed using Eq. (1):

$$HHV_{bio-oil} = 0.3383C + 1.422(H - O/8) \quad (1)$$

where C, H, O are the carbon, hydrogen and oxygen contents.

Evolved pyrolysis gases were quantified using a combined Differential Thermogravimetric-Mass Spectrometry (TG/DTG–MS) system from Perkin Elmer and Balzers [25].

Following the mass balance of the pyrolysis step, the resulting MSW biochar was gasified in a stainless-steel reactor, either alone or blended with CO_2 sorbents at Ca/C molar ratios of 1 or 2. The furnace heating rate remained 10 °C/min, while the final temperature varied between 650 °C and 900 °C. Each run lasted 1 h to ensure complete conversion. Steam was introduced via an automated syringe pump supplying de-ionized water, providing a steam-to-

biochar ratio of 1–3. A 2 m coiled tube surrounding the reactor ensured even steam distribution. The exiting gas stream was first cooled in a cold trap and then dried with silica gel. Gas samples were periodically collected with a Polytetrafluoroethylene (PTFE) Luer-Lock syringe and analyzed using the same TG/DTG–MS system referenced earlier. All experiments were performed in duplicate or more, and the averaged values are reported.

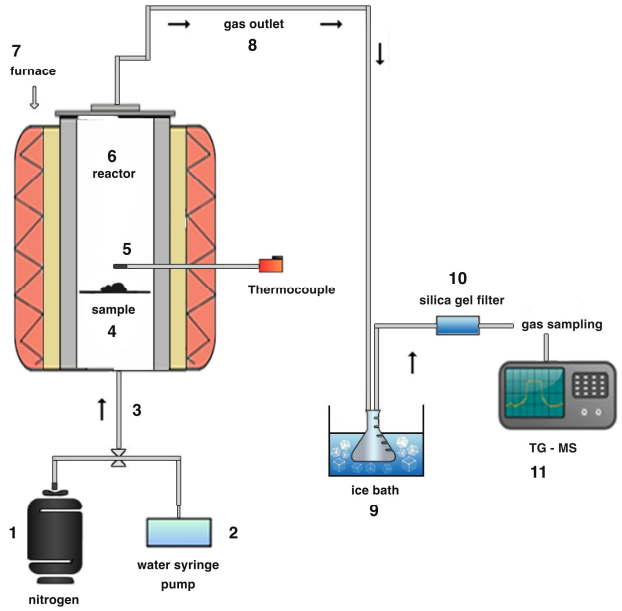

Fig. 1. Experimental setup. 1: Nitrogen gas for pyrolysis tests (Flow rate 200 mL/min). 2: Water syringe pump for gasification tests (Flow rate adjusted for steam/sample 1, 1.5, 2, 2.5, 3, 3.5). 3: Inlet gas or water. 4: Grid sample holder. 5: NiCrNi thermocouple (20 mm above sample bed). 6: Stainless steel fixed bed reactor (ID = 70 mm, H = 140 mm) surrounded by a 2 m pipe for steam flow. 7: Furnace operated up to 900 °C at 10 °C/min. 8: Product gas outlet. 9: Ice bath for condensable volatiles. 10: Silica gel filter for gas drying/gas sampling by PTFE syringe. 11: TG/DTG-MS system for quantitative gas analysis.

The yields of syngas (Y_{syn}) and hydrogen (Y_{H2}) were calculated according to Eq. (2) and Eq. (3):

$$Y_{syn} = x_{syn} \times V_g \quad (2)$$

$$Y_{H2} = x_{H2} \times V_g \quad (3)$$

where x_{syn} and x_{H2} denote the volume fractions of syngas and hydrogen in the product gas mixture, and V_g represents the total volume of gas (m^3).

The Energy Recovery (ER) was determined by Eq. (4):

$$ER = \left(GY \times HHV_g\right)/HHV_b \quad (4)$$

where GY represents the total yield of gas (m^3/kg), and HHV_g, HHV_b represent the higher heating value of product gas (MJ/m^3) and solid char (MJ/kg), respectively.

III. Results and Discussion

A. Characterization of MSW Feedstock and CO_2 Sorbent Materials

Table 1 compares the proximate and ultimate analyses of raw MSW and its char, shows that most of the organic matter in MSW was volatile. After pyrolysis, the hydrogen and oxygen contents were lowered, due to the thermal breakdown of hydrogen- and oxygen-containing organic compounds and the material was enriched in minerals, which both resulted in a reduction of the calorific value. The sulfur and nitrogen contents of the char were low, implying no toxic emissions during the gasification process. Also, from Table 1, it can be observed that after evolution of volatiles during pyrolysis the pore volume of MSW increased and the specific surface area of the char became 6 times higher than that of raw fuel, revealing an increase in its reactivity.

Table 1. Proximate and ultimate analyses, structural characteristics of the fuel

Sample	Volatile Matter	Fixed Carbon	Ash	C	H	N	O	S	HHV (MJ/kg)	Pore Volume × 10^2 (cm^3/g)	Specific Surface Area (m^2/g)
MSW	72.9	1.0	26.1	38.6	6.0	1.3	27.8	0.2	17.0	1.05	8.8
MSW_{char}	-	51.0	49.0	37.4	1.0	1.2	11.3	0.1	12.0	4.55	49.8

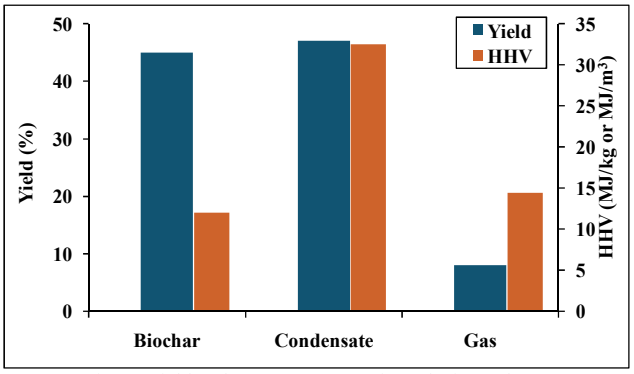

Fig. 2. Yield and energy content of pyrolysis products.

The energy value of the by-products during the pyrolysis step is essential, due to the endothermic nature of the gasification process under study. Fig. 2 shows that the bio-oil and pyrolytic gas, having higher heating values of 32.5 MJ/kg and 14.4 MJ/m^3, respectively, are valuable energy sources for the process. Following the mass balance performed during the pyrolysis process (24% of bio-oil and 8% of gas), the bio-oil could offer about 7800 MJ/t of MSW fuel and the pyrolytic gas about 600 MJ/t of MSW fuel.

The FTIR spectrum of MSW biochar is illustrated in Fig. 3.

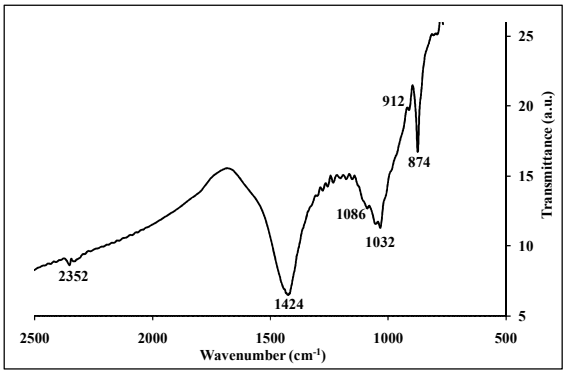

Fig. 3. FTIR spectrum of MSW char.

The small peaks obtained at wave numbers in the range of 500–900 cm^{-1} are assigned to C-H bending groups from

substituted benzene derivatives. The broad band at 1032 cm^{-1} is attributed to C-O stretching from ethers, while the pronounced peak identified at 1422 cm^{-1} corresponds to the -OH bending vibrations, typically associated with alcohols or carboxylic acids. Finally, the small peak at 2354 cm^{-1} corresponds to O=C=O stretching from carbon dioxide. These data confirm the oxygenated organic nature of MSW biochar.

The chemical composition of the CO_2 sorbent materials used in the current study is indicated in Table 2. All solids were rich in calcium and silicon compounds, with the exception of BW, the concentration of which in CaO was 94.5%. FA was also enriched in Al_2O_3 (8.6%), SiO_2 (18.9%) and Fe_2O_3 (7.4%), MSWA had a significant concentration in SiO_2 (21.7%) and to a lesser extent in K_2O (5.8%), whereas OKA contained significant amounts of alkali K and Na (17%), as well as of SiO_2 (12.6%) and P_2O_5 (9%). The XRD spectra represented in Fig. 4 are in agreement with the chemical analysis of the sorbent materials. BW consisted mainly of portlandite, calcite and aragonite minerals. In the FA, calcium was predominantly present as portlandite, lime, calcite and anhydrite, silicon as quartz, whereas aluminum and iron were present in the forms of muscovite and hematite. In MSW, calcium was incorporated in calcite, anhydrite, portlandite and hydroxyapatite, whereas silicon in quartz. In the case of OKA, the principal minerals incorporating calcium were calcite, dolomite and anhydrite, those incorporating potassium were arcanite, sylvite and fairchildite, while the speciations of silicon and phosphorus were identified in quartz and hydroxyapatite.

Table 2. Chemical analysis of CO_2 sorbents (%)

Sample	CaO	Al_2O_3	SiO_2	Fe_2O_3	MgO	K_2O	Na_2O	P_2O_5
BW	94.5	1.9	3.0	0.3	0.2	0.1	-	-
FA	42.2	8.6	18.9	7.4	4.5	0.6	0.5	0.2
MSWA	34.1	3.6	21.7	2.4	3.5	5.8	3.1	2.4
OKA	27.5	1.8	12.6	2.2	5.6	14.1	2.9	9.0

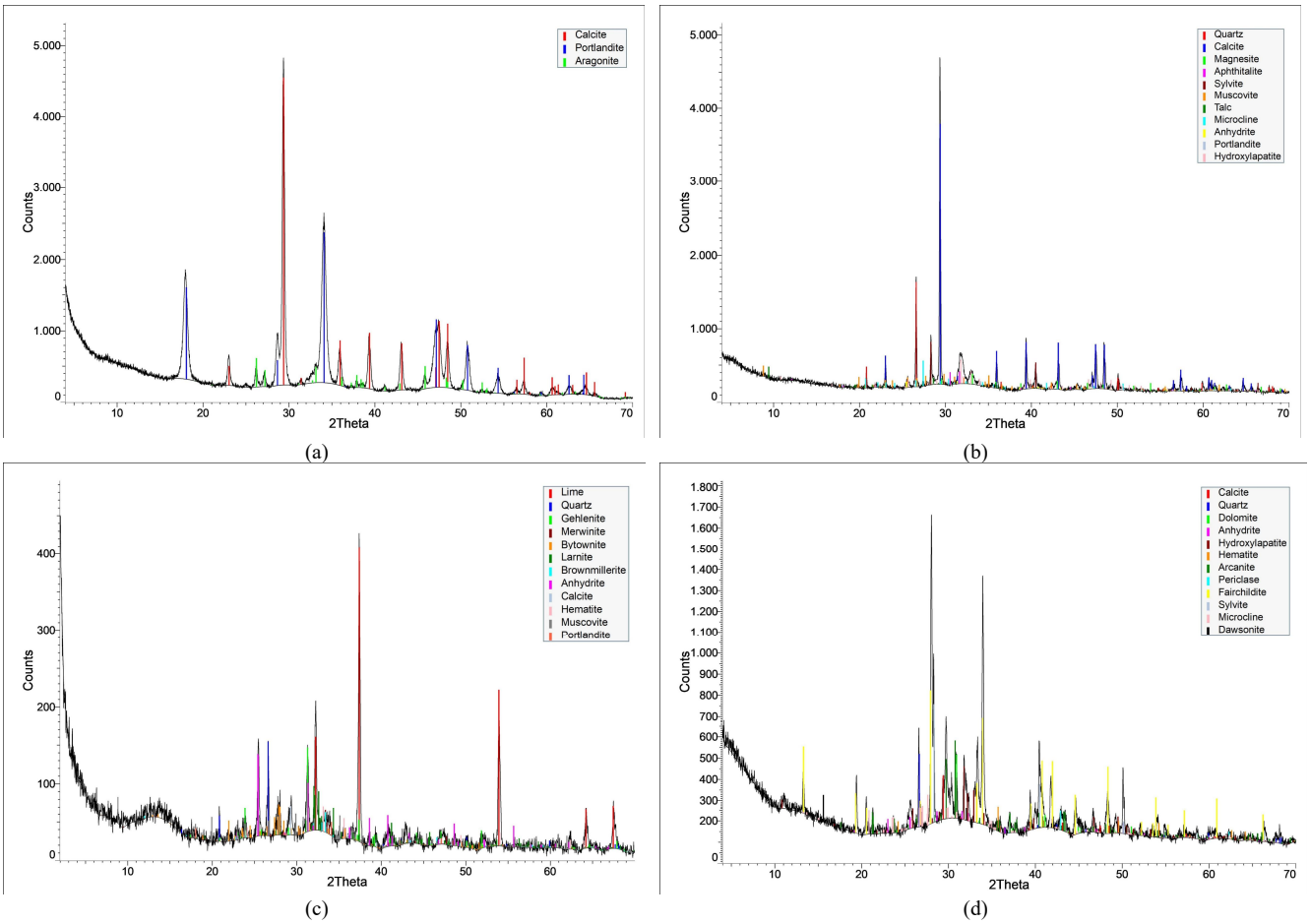

Fig. 4. XRD spectra. (a) BW. (b) MSWA. (c) FA. (d) OKA.

B. Gasification Performance of MSW under Steam without Addition of CO_2 Sorbents

Aiming to investigate the effect of steam-to-biochar ratio on the syngas and hydrogen concentration in the resulting gas mixture, this ratio was varied between 1 and 3, and the results are shown in Fig. 5. The basic reactions of the process are the solid-gas Eqs. (5–8), and the gas-phase Eq. (9) and Eq. (10). It is apparent that as the steam-to-biochar ratio increased from 1 to 3 the concentrations of H_2 and CO_2 in the gas mixture were enhanced, while that of CO was reduced. The yield of H_2 (39 mol% at steam/biochar = 3, 26 mol% at steam/biochar = 1) was nearly doubled, suggesting that endothermic Eq. (5) and Eq. (6) and water-gas shift Eq. (9) presented below, were promoted when the steam flow was higher. Intermediate ratios of 1.5, 2.5 and 3.5 tested, resulted in 28 mol%, 34 mol% and 38.7 mol% H_2, respectively, in the product gas. Accordingly, a steam-to-biochar ratio of 3 was selected as the optimum for subsequent tests.

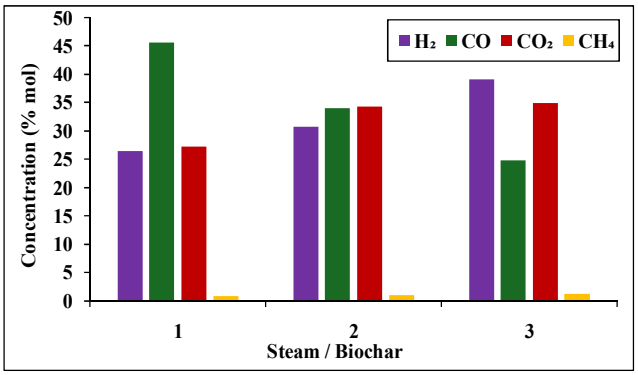

Fig. 5. Effect of steam/biochar on gas composition at 750 °C.

$$C + H_2O \rightarrow CO + H_2 \quad (5)$$

$$C + 2H_2O \rightarrow CO_2 + 2H_2 \quad (6)$$

$$C + CO_2 \rightarrow 2CO \quad (7)$$

$$C + 2H_2 \rightarrow CH_4 \quad (8)$$

$$CO + H_2O \leftrightarrow CO_2 + H_2 \quad (9)$$

$$CH_4 + H_2O \leftrightarrow CO + 3H_2 \quad (10)$$

The temperature-dependent distribution of gaseous products up to 900 °C, along with the H_2/CO molar ratio, the gas higher heating value and fuel conversion efficiency, are depicted in Fig. 6 and Table 3. It is clearly shown from these results that temperature was a critical parameter for the process. As the temperature gradually increased from 650 °C to 900 °C, the concentration of H_2 in the product gas was greatly enhanced, from 10.8 mol% to 51.8 mol%. On the contrary, the content of CO dropped significantly from 74.3 mol% at 650 °C to 27.1 mol% at 900 °C, while that of CO_2 attained a maximum value of 42 mol% at 800 °C. The amount of CH_4 was very low at all temperatures, because Eq. (8) proceeds only at elevated pressures. According to the primary reactions taking place simultaneously within the reactor, these findings indicate that Eq. (5), Eq. (6), Eq. (9), and the reverse of Eq. (10) were thermodynamically favoured. Also, although Eq. (7) was promoted above 700 °C, the CO produced was consumed through Eq. (9) and Eq. (10), confirming its reduction with temperature.

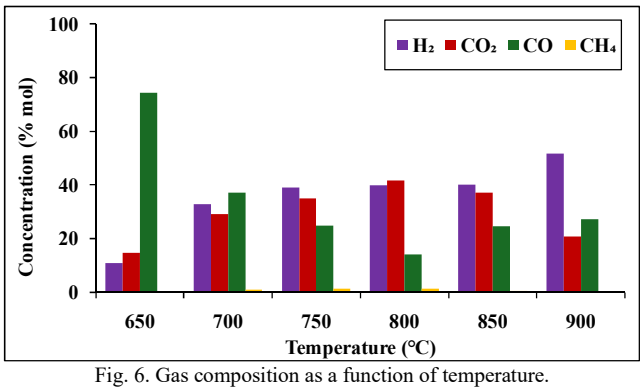

Fig. 6. Gas composition as a function of temperature.

Table 3. Gasification performance of fuel without addition of CO_2 sorbents

Temperature (°C)	H_2/CO (mol/mol)	HHV (MJ/m³)	GE (%dry)
650	0.14	12.3	9.0
700	0.89	9.4	23.1
750	1.57	8.5	34.0
800	2.80	7.5	41.6
850	1.64	8.6	45.9
900	1.90	10.3	47.7

The enrichment of product gas in CO_2 somehow reduced its higher heating value, as the temperature increased. The highest H_2/CO molar ratio was achieved at 800 °C (Table 3) and it was 2.8. Fuel conversion was raised with temperature, due to the promotion of the endothermic gasification reactions, reaching a value of 47.7% at 900 °C, on a dry basis. Nearly complete conversion of the organic matter in MSW was achieved at this temperature, reaching 93.5%.

C. Gasification Performance of MSW under Steam with Addition of CO_2 Sorbents

The composition of product gas, its higher heating value and the H_2/CO molar ratio as a function of temperature and Ca/C molar ratio, when BW was used as a CO_2 sorbent, are summarized in Table 4. CO_2 was captured according to Eq. (11):

$$Ca(OH)_2 + CO_2 \leftrightarrow CaCO_3 + H_2O \quad (11)$$

A final gasification temperature of 750 °C was selected, as above this temperature calcium carbonate starts to decompose, thus enriching the gas in CO_2. When Ca/C = 1, the concentration of hydrogen in the gas mixture was increased by 96.9%, reaching a value of 76.8 mol%. BW material captured 92.6% of CO_2. When Ca/C = 2, the percentage of H_2 in the gas was even higher 80.8%, however, the sorbent was somehow saturated, so that no further reduction of CO_2 occurred. The enrichment of product gas in hydrogen and the reduction of CO in the presence of the sorbent were reflected in the H_2/CO molar ratio, which attained a maximum value of 5.46 at a Ca/C = 2, suggesting that reactions Eq. (5), Eq. (6), Eq. (9) were favoured in this case. Therefore, according to these results, it can be speculated that the gasification of MSW by steam shows promise as a viable route for biofuel production or for chemical synthesis [33]. Furthermore, Table 4 shows that above 700 °C, the higher heating value of gas produced was raised from 8.5–9.4 MJ/m³ to 12.6–13.9 MJ/m³ in the presence of BW material.

A comparison of the effect of all CO_2 sorbent materials used in this study on the enrichment of product gas in hydrogen, the yield of syngas (CO + H_2), the H_2/CO molar ratio and the energy recovery from the gasification of MSW fuel, at 750 °C and molar ratios Ca/C 1 and 2, is made in Table 5 and Fig. 7. It was evident that the highest hydrogen yield in the gas mixture occurred when BW was used as a CO_2 sorbent, particularly at a Ca/C ratio of 2, by reducing the content of CO_2 by 91.1%.

Table 4. Gasification performance of fuel with addition of BW as a sorbent

Ca/C (mol/mol)	Temperature (°C)	Gas Composition (mol%)					H_2/CO (mol/mol)	HHV (MJ/m³)
		H_2	CO	CO_2	CH_4	C_xH_y		
0	650	10.8	74.3	14.7	0.2	0.09	0.14	12.3
	700	32.8	37.0	29.1	0.9	0.05	0.89	9.4
	730	34.6	31.7	32.6	1.0	0.05	1.09	8.9

	750	39.0	24.8	34.9	1.2	0.05	1.67	8.5
1	650	27.0	72.4	0.4	0.13	0.10	0.37	12.8
	700	57.3	49.8	0.5	0.57	0.06	1.15	13.9
	730	58.6	39.5	1.0	0.93	0.04	1.48	12.9
	750	76.8	19.0	2.6	1.54	0.04	4.0	12.6
2	650	35.5	64.3	0.04	0.11	0.06	0.55	12.8
	700	61.4	37.6	0.5	0.51	0.02	1.63	12.8
	730	72.8	25.2	1.1	0.89	0.02	2.89	12.9
	750	80.8	14.8	3.1	1.27	0.07	5.46	12.7

Table 5. Comparison of CO_2 sorbents effect on gasification performance of fuel at 750 °C

Sorbent	Ca/C (mol/mol)	Gas Composition (mol%)					HHV (MJ/m³)	Syngas Yield (m³/kg)	ER
		H_2	CO	CO_2	CH_4	C_xH_y			
BW	1	76.8	19.0	2.6	1.5	0.04	12.6	0.93	1.02
	2	80.8	14.8	3.1	1.3	0.02	12.7	1.05	1.06
FA	1	56.3	37.5	4.8	1.3	0.06	12.5	0.55	0.61
	2	65.0	30.3	3.1	1.6	0.03	12.7	0.68	0.76
MSWA	1	60.9	34.4	3.5	1.2	0.04	12.7	0.62	0.69
	2	64.0	32.0	3.1	0.9	0.05	12.6	0.67	0.73
OKA	1	52.8	33.4	13.2	0.5	0.13	11.3	0.42	0.46
	2	56.6	33.9	8.8	0.6	0.05	11.8	0.50	0.54

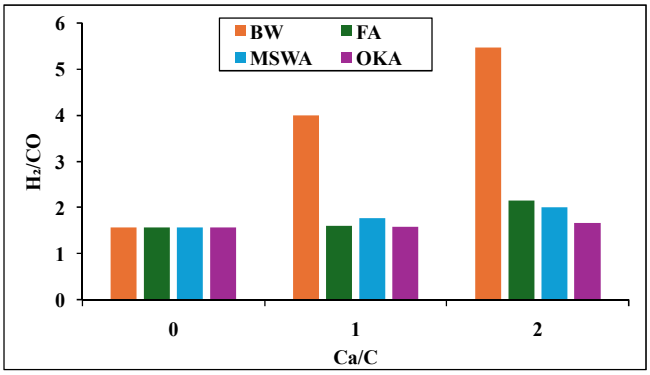

Fig. 7. Effect of Ca/C of sorbents on H_2/CO at 750 °C.

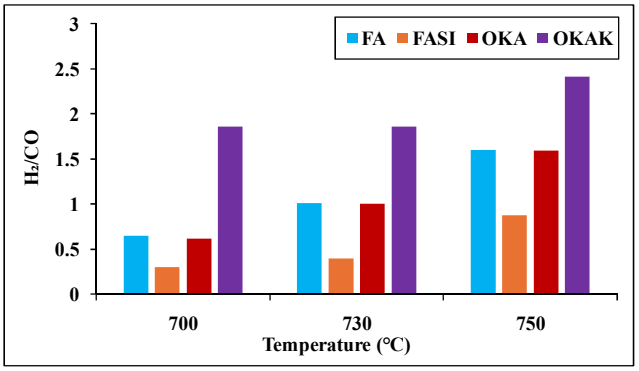

Fig. 8. Effect of Si and K of FA and OKA sorbents on H_2/CO.

The H_2/CO molar ratio was very high, 5.46 under these conditions, the syngas yield was maximized (1.05 m³/kg), the heating value of the gas (12.7 MJ/m³), leading to the highest energy recovery, as compared to the other sorbent materials. The poorest performance was obtained in the case of OKA as a sorbent (CO_2 capture 74.8%). These findings can be explained by the higher amount of calcium in the BW material in the form of portlandite, the active sorbent of CO_2 according to Eq. (11), which was 50% of the raw material, prior to water saturation (the specific surface area of this material was 0.55 m²/g, as measured by the Autosorb analyzer).

In order to investigate the lower performance of OKA and FA in terms of hydrogen production and CO_2 capture, 2 different ash samples containing about the same CaO as the original ones, but higher potassium (30% K_2O instead of 14.1% for OKA) and silicon (38% SiO_2 instead of 18.9% for FA) contents respectively, were tested at different temperatures and their influence on the H_2/CO molar ratio is compared in Fig. 8. It is obvious that a higher amount of potassium, which was identified as carbonate (arcanite) in the OKA ash and a higher amount of silicon as quartz in FA, significantly increased or lowered the hydrogen content of the product gas, respectively. Therefore, K_2CO_3 played a catalytic role by promoting endothermic reactions and the water-gas shift (Eq. (9)). This effect was likely due to its ability to increase the number of active sites on the char surface or alter the nature and reactivity of surface intermediates, as supported by findings in prior research [34]. A possible mechanism [34, 35] is described by Eqs. (12–14):

$$K_2CO_3 + 2C \rightarrow 2K + 3CO \quad (12)$$

$$2K + 2H_2O \rightarrow 2KOH + H_2 \quad (13)$$

$$2KOH + CO \rightarrow K_2CO_3 + H_2 \quad (14)$$

Conversely, the enrichment of silicon in the fly ash, in the form of inactive quartz, led to the reduction of the gasification rate and consequently the reactivity of the carbon-steam endothermic reactions, thus confirming its inhibitory effect on the gasification of the char [19, 36].

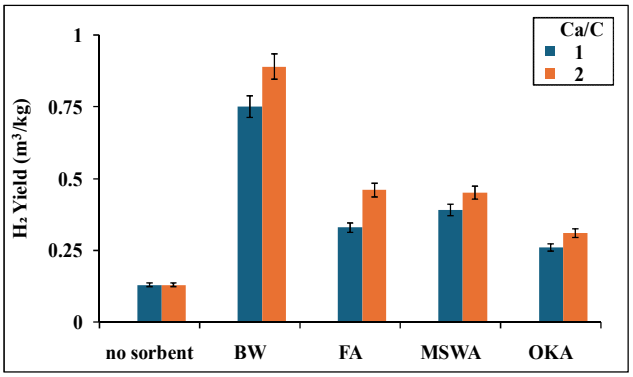

Fig. 9. Effect of Ca/C of sorbents on hydrogen yield at 750 °C.

A highly important criterion for evaluating the gasification performance of various feedstocks is the highest possible generation of combustible gas or hydrogen. Fig. 9 compares the yield of hydrogen without or with the addition of CO_2 sorbent materials at 750 °C, with respect to the Ca/C molar ratio. Obviously, as also supported by the results presented

above, the greater volume of syngas produced, when BW was used as sorbent, contributed to the highest hydrogen yield during the process, which was about 7 times higher than the one obtained without any CO_2 sorbent.

The steam gasification of MSW has not been extensively studied in past investigations. The wide range of experimental conditions and configurations used, generating different results, as well as the variability in the interpretation of the results, makes the comparison with the present data difficult. The comparison must be limited to the steam gasification of MSW in fixed bed systems. Some studies have reported H_2 and CO concentrations in syngas ranging from 32–57 mol% and 15–17 mol%, respectively, at temperatures 800–900 °C without the addition of any CO_2 sorbent, which agrees with current findings [5, 31]. Furthermore, the average composition of the syngas from high temperature gasification (>1100 °C) of MSW has been reported to be 37–39 vol% H_2 and 40–41 vol% CO [26]. The steam gasification of refused-derived fuel at 900 °C and a steam/refused-derived fuel mass ratio of 1, in a fixed bed reactor, generated approximately 36 mol% H_2 and 32 mol% CO [20]. These data also agree with the present results. When waste marble or CaO was used to capture CO_2 from the gas at waste marble/MSW = 1 and Ca/C = 0.7 respectively [5, 30], the percentage of hydrogen in the mixture was found to be 28% and 49.4% respectively, at 750 °C, while that of CO_2 was high (up to 30 mol%). For a mixture of MSW and wood residue, at a ratio of 1:1.25 with the addition of CaO at 2:1 and 0.92:1, a thermodynamic simulation predicted 68.8 mol% H_2/kg feed and a CO_2 capture efficiency of 92% [22]. On the other hand, when gypsum was used as a CO_2 sorbent at gypsum/MSW = 1, the yield of syngas at 800 °C was lowered by 50% [16]. Therefore, the formation of hydrogen or syngas as products of MSW gasification, under the conditions of the present work in the presence of various waste materials as CO_2 sorbents, is far superior to literature data.

IV. Conclusions

MSW char had a high content of ash and its organic matter was oxygenated to a great extent. CO_2 sorbents were rich in calcium, with BW consisting mostly of portlandite mineral. The optimum steam-to-biochar ratio during the tests was 3. During the steam gasification of MSW without the addition of sorbent materials up to 900 °C, the concentration of H_2 in the product gas reached a value of 51.8 mol%, while that of CO_2 increased up to 42 mol%. The organic matter was almost completely converted.

When BW was used as a CO_2 sorbent, the highest percentage of H_2 in the gas mixture was achieved at 750 °C and Ca/C = 2, 80.8 mol%, 91.1% of CO_2 was captured, H_2/CO was 5.5, H_2 yield 0.89 m^3/kg and energy recovery 1.06. The poorest performance was obtained in the case of OKA as a sorbent (CO_2 capture 74.8%). A higher amount of potassium in the form of carbonate in OKA increased the reactivity of MSW, while a higher amount of silicon in FA as quartz had the opposite effect.

Overall, in alignment with the circular economy and mitigation of carbon footprint to the environment, the steam gasification of municipal solid wastes in the presence of waste materials rich in calcium was proved to be successful, producing a gas rich in hydrogen, up to 80.8 mol% and capturing up to 92.6% of CO_2 emissions.

Conflict of Interest

The authors declare no conflict of interest.

Author Contributions

Conceptualization: D.V.; methodology: D.V.; software: K.K., S.K., A.S.; validation: K.K., D.V.; writing—original draft preparation: D.V.; writing—review and editing D.V.. All authors had approved the final version.

Acknowledgment

The authors kindly thank the laboratories of Inorganic and Organic Geochemistry, Hydrocarbons Chemistry and Prof. G. Xiroudakis of the Technical University of Crete, as well as Dr. T. Ioannides and Dr. M. Smyrnioti from the Inst. of Chemical Engineering Sciences in Patra, for the various analyses of the samples.

References

[1] A. T. Sipra, N. Gao, and H. Sarwar, "Municipal solid waste (MSW) pyrolysis for biofuels production: A review of effects of MSW components and catalysts," *Fuel Process. Technol*., vol. 175, pp. 131–147, 2018.

[2] T. G. Ambaye, R. Djellabi, M. Vaccari *et al.*, "Emerging technologies and sustainable strategies for municipal solid waste valorization: Challenges of circular economy implementation," *J. Clean. Prod.*, vol. 423, Art. no. 138708, 2023.

[3] A. Kaur, R. Bharti, and R. Sharma, "Municipal solid waste as a source of energy," *Materials Today: Proc*., vol. 81, pp. 904–915, 2023.

[4] D. J. Lee, "Gasification of municipal solid waste (MSW) as a cleaner final disposal route: A mini-review," *Biores. Technol*., vol. 344, Art. no. 126217, 2022.

[5] M. Irfan, A. Li, L. Zhang *et al.*, "Production of hydrogen enriched syngas from municipal solid waste gasification with waste marble powder as a catalyst," *Int. J. Hydr. Energy*, vol. 44, pp. 8051–8061, 2019.

[6] G. Chen, I. A. Jamro, S. R. Samo *et al.*, "Hydrogen-rich syngas production from municipal solid waste gasification through the application of central composite design: An optimization study," *Int. J. Hydr. Energy,* vol. 45, pp. 33260–33273, 2020.

[7] Y. A. Situmorang, Z. Zhao, N. Chaihad *et al.*, "Steam gasification of co-pyrolysis chars from various types of biomass," *Int. J. Hydr. Energy*, vol. 46, pp. 3640–3650, 2021.

[8] N. Amin, Z. Khan, A. Razzaq *et al.*, "Municipal solid waste air gasification using waste marble powder as a catalyst for syngas production," *J. Energy Inst.*, vol. 113, Art. no. 101496, 2024.

[9] A. Ramos, E. Monteiro, V. Silva *et al.*, "Co-gasification and recent developments on waste-to-energy conversion: A review," *Renew. Sust. Energy Rev.*, vol. 81, pp. 380–396, 2018.

[10] Z. Hameed, M. Aslam, Z. Khan *et al.*, "Gasification of municipal solid waste blends with biomass for energy production and resources recovery: Current status, hybrid technologies and innovative prospects," *Renew. Sust. Energy Rev*., vol. 136, Art. no. 110375, 2021.

[11] Y. Qi, U. Muhammad, W. Zhang *et al.*, "A comprehensive evaluation of recent advancement in municipal solid waste gasification: Research status, technical challenges and perspectives," *Separ. Purif.*, *Technol*., vol. 358, Art. no. 130443, 2025.

[12] P. Suhaj, J. Haydary, J. Husar *et al.*, "Catalytic gasification of refuse-derived fuel in a two-stage laboratory scale pyrolysis/gasification unit with catalyst based on clay minerals," *Waste Manag.*, vol. 85, pp. 1–10, 2019.

[13] A. Li, H. Han, S. Hu *et al.*, "A novel sludge pyrolysis and biomass gasification integrated method to enhance hydrogen-rich gas generation," *Energy Conv. Manag.*, vol. 254, Art. no. 115205, 2022.

[14] Y. Tian, W. Liu, C. Zeng *et al.*, "Experimental study on steam co-gasification of biomass/municipal solid waste (MSW) for H_2-rich gas production," *J. Energy Inst*., vol. 118, Art. no. 101931, 2025.

[15] A. M. Ali, M. Shahbaz, M. Inayat *et al.*, "Conversion of municipals waste into syngas and methanol via steam gasification using CaO as sorbent: An aspen plus modelling," *Fuel*, vol. 349, Art. no. 128640, 2023.

[16] K. R. G. Burra, I. F. Hernandez, M. J. Castaldi *et al.*, "Gasification of municipal solid wastes with gypsum wastes under different gasifying environments," *J. Energy Inst*., vol. 114, Art. no. 101644, 2024.
[17] G. Centi and S. Perathoner, "Chemistry and energy beyond fossil fuels. A perspective view on the role of syngas from waste sources," *Catal. Today*, vol. 342, pp. 4–12, 2020.
[18] F. Wang, L. Wang, A. M. Sadeq *et al.*, "Biomass gasification combined with a novel heat integration design for sustainable energy supply programs: Comprehensive thermodynamic, environmental and economic evaluations," *Energy*, vol. 337, Art. no. 138560, 2025.
[19] S. Aluri, A. Syed, D. W. Flick *et al.*, "Pyrolysis and gasification studies of model refuse derived fuel (RDF) using thermogravimetric analysis," *Fuel Proc. Technol*., vol. 179, pp. 154–166, 2018.
[20] J. Cai, R. Zeng, W. Zheng *et al.*, "Synergistic effects of co-gasification of municipal solid waste and biomass in fixed-bed gasifier," *Process Saf. Environ. Prot*., vol. 148, pp. 1–12, 2021.
[21] R. Liang, C. Chen, Y. Ge *et al.*, "A conceptual sorting strategy of municipal solid waste towards efficient gasification," *Energy Conver. Manag*., vol. 304, Art. no. 118209, 2024.
[22] A.V. Bagde and M. C. Paul, "Waste to hydrogen: Steam gasification of municipal solid wastes with carbon capture for enhanced hydrogen production," *Biomass Bioenergy*, vol. 198, Art. no. 107855, 2025.
[23] S. Vikram, S. P. Deore, C. D. Blasio *et al.*, "Air gasification of high-ash solid waste in a pilot-scale downdraft gasifier: Experimental and numerical analysis," *Energy*, vol. 270, Art. no. 126912, 2023.
[24] A. Saravanakumar, M. R. Sudha, V. Pradeshwaran *et al.*, "Green circular economy of co-gasification with municipal solid waste and wood waste in a novel downdraft gasifier with rotating grade," *Chem. Eng. J.*, vol. 479, Art. no. 147987, 2024.
[25] D. Vamvuka, E. Afthentopoulos, and S. Sfakiotakis, "H_2-rich gas production from steam gasification of a winery waste and its blends with industrial wastes. Effect of operating parameters on gas quality and efficiency," *Renew. Energy*, vol. 197, pp. 1224–1232, 2022.
[26] A. Borgogna, G. Centi, G. Iaquaniello *et al.*, "Assessment of hydrogen production from municipal solid wastes as competitive route to produce low-carbon H_2," *Sci. Tot. Environ.*, vol. 827, Art. no. 154393, 2022.
[27] J. You, X. Chen, Y. Huang *et al.*, "Hydrogen-rich gas production from catalytic steam-gasification of municipal solid waste: Product gas upgrading by in-bed use of olivine," *J. Energy Inst*., vol. 122, Art. no. 102221, 2025.
[28] B. A. Saputro, H. Dafiqurrohman, N. K. Supriatna *et al.*, "Steam gasification of municipal solid waste using Fe2O3/Al2O3 and zeolite catalysts in a fixed-bed gasifier for hydrogen-rich syngas production," *Int. J. Hydr. Energy*, vol. 158, Art. no. 150446, 2025.
[29] M. Irfan, A. Li, L. Zhang *et al.*, "Enhanced hydrogen production from municipal solid waste gasification using Ni-CaO-TiO_2 bifunctional catalyst prepared by de arc plasma melting," *Ind. Eng. Che. Res*., vol. 58, pp. 13408–13419, 2019.
[30] M. Hu, D. Guo, C. Ma *et al.*, "Hydrogen rich gas production by the gasification of wet MSW coupled with carbon dioxide capture," *Energy*, vol. 90, pp. 857–863, 2015.
[31] X. Zeng, M. Fang, T. Lv *et al.*, "Enhanced hydrogen production by the catalytic alkaline thermal gasification of cellulose with Ni/Fe dual-functional CaO based catalysts," *Int. J. Hydr. Energy*, vol. 46, pp. 32783–32799, 2021.
[32] D. Vamvuka, S. Sfakiotakis, and M. Galetakis, "Catalytic co-gasification of refuse derived fuel and industrial waste biomass under steam using a novel waste material as CO_2 sorbent," *IJISET*, vol. 12, pp. 4–15, 2025.
[33] G. Nagy and Z. Dobo, "Experimental investigation of fixed-bed pyrolysis and steam gasification of food waste blended with woody biomass," *Biomass Bioenergy,* vol. 139, Art. no. 105580, 2020.
[34] S. Ning, S. Jia, H. Ying *et al.*, "Hydrogen-rich syngas produced by catalytic steam gasification of corncob char," *Biomass Bioenergy*, vol. 117, pp. 131–136, 2018.
[35] A. Sinag, A. Kruse, and V. Schwarzkopf, "Key compounds of the hydropyrolysis of glucose in supercritical water in the presence of K_2CO_3," *Ind. Eng. Chem. Res*., vol. 42, pp. 3516–3521, 2003.
[36] M. Elsaddik, A. Nzihou, M. Delmas *et al.*, "Steam gasification of cellulose pulp char: Insights on experimental and kinetic study with a focus on the role of silicon," *Energy,* vol. 271, Art. no. 126997, 2023.